JB
Journals.ASM.org

Identification and Characterization of Five Intramembrane Metalloproteases in *Anabaena variabilis*

Kangming Chen, Liping Gu, Xianling Xiang,* Michael Lynch, and Ruanbao Zhou

Department of Biology and Microbiology, South Dakota State University, Brookings, South Dakota, USA

Regulated intramembrane proteolysis (RIP) involves cleavage of a transmembrane segment of a protein, releasing the active form of a membrane-anchored transcription factor (MTF) or a membrane-tethered signaling protein in response to an extracellular or intracellular signal. RIP is conserved from bacteria to humans and governs many important signaling pathways in both prokaryotes and eukaryotes. Proteases that carry out these cleavages are named intramembrane cleaving proteases (I-CLips). To date, little is known about I-CLips in cyanobacteria. In this study, five putative site-2 type I-Clips (Ava_1070, Ava_1730, Ava_1797, Ava_3438, and Ava_4785) were identified through a genome-wide survey in *Anabaena variabilis*. Biochemical analysis demonstrated that these five putative *A. variabilis* site-2 proteases (S2Ps$_{Av}$) have authentic protease activities toward an artificial substrate pro-σ^K, a *Bacillus subtilis* MTF, in our reconstituted *Escherichia coli* system. The enzymatic activities of processing pro-σ^K differ among these five S2Ps$_{Av}$. Substitution of glutamic acid (E) by glutamine (Q) in the conserved HEXXH zinc-coordinated motif caused the loss of protease activities in these five S2Ps$_{Av}$, suggesting that they belonged to the metalloprotease family. Further mapping of the cleaved peptides of pro-σ^K by Ava_4785 and Ava_1797 revealed that Ava_4785 and Ava_1797 recognized the same cleavage site in pro-σ^K as SpoIVFB, a cognate S2P of pro-σ^K from *B. subtilis*. Taking these results together, we report here for the first time the identification of five metallo-intramembrane cleaving proteases in *Anabaena variabilis*. The experimental system described herein should be applicable to studies of other RIP events and amenable to developing *in vitro* assays for I-CLips.

Regulating the activity of transcription factors is an efficient way to regulate gene expression. In addition to several well-known mechanisms for regulating the activity of transcription factors, such as posttranslational modifications (23, 27) and degradation of an antitranscription factor or its antagonistic protein (3, 15, 21), a recently discovered and little-understood regulation is intramembrane proteolysis of membrane-tethered transcription factors. Spatiotemporal sequestration of transcription factors in the cellular membrane is emerging as an elegant mechanism for the regulation of gene expression. The regulated intramembrane proteolysis (RIP) of membrane-tethered transcription factors (MTFs) (8, 35, 56) or membrane-anchored signaling proteins (MSPs) (12, 57, 59) by membrane-embedded proteases plays important roles in eliciting transcriptional responses in many vital cellular processes, including cell division and differentiation (6, 12, 48, 51, 66), cell migration (60), stress responses (3, 15, 26, 64), microbial pathogenesis (5, 40–42, 45), cholesterol biosynthesis (47), and human innate and adaptive immunity (20), as well as pathogenesis of cancer (4, 34, 39) and human diseases such as hyperlipidemias and Alzheimer's (51, 53). Since RIP-mediated signal transduction does not require *de novo* protein synthesis due to sequestration of transcription factors in the cellular membrane, this allows the signal to be transmitted across cell membranes quickly in response to an extracellular or intracellular signal. Furthermore, the MTF itself serves as both a signal transducer and a trigger of target gene expression in an RIP signaling pathway. Another unique feature of RIP is that intramembrane-cleaving proteases (I-CLips) with catalytic-site motifs embedded within transmembrane (TM) segments (2, 17, 19, 61) cleave the transmembrane helix (TMH) of an MTF or MSP inside the lipid bilayer, a hydrophobic environment that is quite different from the aqueous environment required for conventional proteolytic enzymes. Thus, I-CLips can accomplish many important membrane-involved tasks beyond the capability of their soluble cousins. How this membrane-mediated proteolysis occurs is an unanswered question in the study of the enzymology and membrane biology of I-CLips.

Typically, a two-step cleavage pattern is employed in RIP (7). An initial cleavage by site-1 protease (S1P) at a site outside the membrane generates a shortened peptide of a MTF, which is a prerequisite for the next cleavage. Then a site-2 protease (S2P) activates the MTF by cleavage of its transmembrane segment to release the transcriptional activation domain (TAD) from the membrane, allowing it to regulate downstream target genes (Fig. 1). Proteases that carry out these cleavages are called I-CLips (59). Three well-known families of I-CLips have been documented; they are intramembrane aspartyl proteases (e.g., presenilins and signal peptide peptidase [SPP]) (11, 37), rhomboid serine proteases (24, 54), and S2P metalloproteases (7). Among them, RIP by S2P metalloproteases has been found in both prokaryotes and eukaryotes. For example, S2P-SREBP (sterol regulatory-element-binding protein) RIP from *Homo sapiens*, the first identified RIP pair, plays an important role in regulation of sterol and fatty acid synthesis and uptake through RIP activation of SREBP (7). The SREBP precursor is sequestrated to the endoplasmic reticulum

Received 28 July 2012 **Accepted** 31 August 2012
Published ahead of print 7 September 2012
Address correspondence to Ruanbao Zhou, Ruanbao.Zhou@sdstate.edu.
* Present address: Xianling Xiang, College of Life Sciences, Anhui Normal University, Wuhu, China.
Supplemental material for this article may be found at http://jb.asm.org/.

doi:10.1128/JB.01366-12

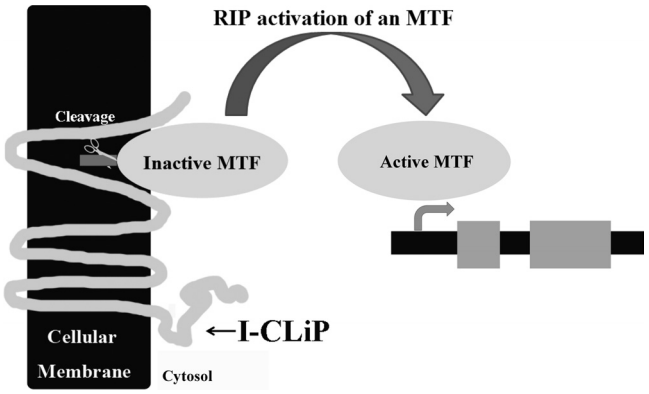

FIG 1 Diagram illustrates the typical regulated intramembrane proteolytic (RIP) activation of the membrane-anchored transcription factor in the cell. Inactive MTF (membrane portion shown in dark gray and cytosolic portion in light gray) is temporally membrane sequestered away from the transcription machinery. In quick response to an extracellular or intracellular signal, MTF undergoes an intramembrane proteolytic activation by an I-CLip, releasing an active MTF access to the transcription machinery to timely regulate target gene expressions.

(ER) after it is synthesized. Under low-cholesterol conditions, SREBP is transported to the Golgi apparatus from the ER by COPII-coated transport vesicles (16, 55). In the Golgi apparatus, SREBP first must be cleaved by a serine protease site-1 protease around the consensus sequence RXXL in the luminal loop of SREBP (7). Then, this shortened peptide, which is still attached to the membrane, is recognized and attacked by a site-2 protease within the membrane, releasing a transcriptional activation domain to regulate cholesterol biosynthetic genes in the nucleus (7). Finally, this signaling pathway can be inhibited by elevated levels of cholesterol. Another example of an S2P homolog is SpoIVFB in *Bacillus subtilis*, which cleaves the N-terminal membrane segment of pro-σ^K and releases an active σ^K from the forespore membrane into the cytosol of the mother cell, where σ^K turns on the genes required for spore maturation (66, 68, 69). RIP is a well-conserved mechanism that controls many important signaling pathways found in bacteria, fungi, higher plants, and humans (8, 29, 37, 57, 59, 61). Over 1,857 putative S2Ps were identified in available genomes, including the human genome and the genomes of higher plants (http://merops.sanger.ac.uk/cgi-bin/famsum?family=m50). Only five paired S2P RIP systems have been studied to date. They are *B. subtilis* SpoIVFB-pro-σ^K (31, 33, 48, 66, 68, 69) and YluC-RsiW/FtsL (6, 50), *Escherichia coli* RseP-RseA (3), *Caulobacter crescentus* MmpA-PodJ (10), and *H. sapiens* S2P-SREBP/ATF6 (8, 52). There has been no genome-wide study of RIP in any organism so far. Thus, we systematically explore RIP in *Anabaena variabilis* ATCC 29413 (here, *A. variabilis*), a filamentous heterocyst-forming cyanobacterium capable of fixing nitrogen and CO_2 using the energy of sunlight via oxygen-evolving plant-type photosynthesis. In addition, it has four distinct differentiated cell types, including vegetative cells for photosynthesis, heterocysts for nitrogen fixation (22, 62, 63), akinetes (spores) for survival (1, 36, 70), and hormogonia for motility and for the establishment of symbiosis (44, 46). Based on the studies of RIP in other organisms (3, 6, 28, 43, 48), we speculate that RIP in *A. variabilis* may play important roles in the differentiation of heterocysts, akinetes (spores), and hormogonia, in coupling oxygenic photosynthesis and aerobic nitrogen fixation, in stress adaptations, in cell-cell communication, and/or in symbiosis with plants.

In this study, we screened and identified five putative S2Ps in *A. variabilis* ($S2Ps_{Av}$) by a similarity search against the *A. variabilis* genome using *B. subtilis* SpoIVFB as a template. Our experimental data provide strong evidence for the first time that there are five metallo-intramembrane proteases in *A. variabilis*.

MATERIALS AND METHODS

Bacterial strains and plasmids. *E. coli* strains TOP10 (Invitrogen) and NEB10-beta (New England BioLabs) were used for routine maintenance and preparation of plasmids; BL21(DE3) (Novagen) was used for overexpression of recombinant protein. Luria-Bertani (LB) broth was used for the growth of *E. coli*. Antibiotics were used at the following concentrations: ampicillin (Amp), 100 μg/ml; kanamycin (Kan), 50 μg/ml. Each $S2P_{Av}$ open reading frame (ORF) (ava_1070, ava_1730, ava_1797, ava_3438, and ava_4785), as well as the truncated ava_1070 consisting of amino acid residues 201 to 417 [ava_1070(201–417)] and ava_3438(184–407), was amplified from *A. variabilis* genomic DNA using primers described in Table S1 in the supplemental material. Unless otherwise noted, all PCR products were amplified using *Pfu Turbo* DNA polymerase (Stratagene) and cloned into pCR2.1-TOPO vector (TOPO TA Cloning Kit; Invitrogen). Then fragments containing $S2P_{Av}$ genes were excised from the TOPO vector and subcloned into a pET21b-derived vector (Table 1). The expression vector pZR827, which contains a transmembrane segment (denoted cytTM, residues 1 to 23) from rabbit cytochrome P450 2B4 (49) upstream of a multiple cloning site (MCS), was used to generate N-terminal cytTM fusion $S2P_{Av}$ proteins. A pro-σ^K consisting of residues 1 to 126 and with an S20G mutation [pro-σ^K(1-126)S20G] encoded in plasmid pZR327 (67) was used as the artificial substrate for testing the proteolytic activities of $S2Ps_{Av}$. All genes subjected to mutagenesis were carried out using a QuikChange kit from Stratagene. All cloned PCR products and mutated genes were confirmed by DNA sequencing.

Cotransformation of plasmids into *E. coli* and induction of recombinant proteins. To test the proteolytic activities of the five putative $S2Ps_{Av}$ in our reconstituted *E. coli* system, a plasmid bearing an individual $S2P_{Av}$ gene (Amp^r) and plasmid pZR327 bearing the pro-σ^K(1–126)S20G gene (Kan^r) were cotransformed into *E. coli* BL21(DE3). A single colony grown on LB agar plate with antibiotics Amp and Kan was inoculated into 5 ml of LB broth containing Amp and Kan and incubated at 37°C with rotation at 250 rpm until it reached an optical density at 600 nm (OD_{600}) of about 1.0. Expression of the recombinant proteins was induced with isopropyl-β-D-thiogalactopyranoside (IPTG; 250 μM), and incubation was continued at 37°C at 250 rpm for 3 h; then cells were collected by centrifugation and stored at −80°C.

Fractionation of cellular proteins. To determine the subcellular localization of $S2Ps_{Av}$, the whole-cell lysate, cytoplasmic fraction, and membrane fraction were prepared as described previously (68) with the following modifications. *E. coli* cells from 100-ml cultures induced as described above were harvested by centrifugation (12,000 × *g* for 10 min) and resuspended in 6 ml of phosphate-buffered saline (PBS) lysis buffer (pH 7.2) (Invitrogen), containing 1 mM Pefabloc, 0.5 mg/ml lysozyme, 10 μg/ml DNase I, and 10 μg/ml RNase A. Cells were disrupted by passage twice through a Nano DeBEE electric benchtop laboratory homogenizer (BEE International) at 14,000 lb/in^2, and cell debris was separated by centrifugation at 12,000 × *g* for 10 min at 4°C. The low-speed supernatant was subjected to ultracentrifugation at 4°C for 1.5 h at 200,000 × *g* (Optima 130K Ultracentrifuge; Beckman). The resulting ultrasupernatant (4.5 ml) served as the cytoplasmic fraction. The pellet was resuspended in PBS (4.5 ml) with 1% Sarkosyl, and this suspension served as the membrane fraction. Sample preparation was described previously (67, 68). Equal amounts of 2× sample buffer (50 mM Tris-HCl, pH 6.8, 4% SDS, 20% [vol/vol] glycerol, 200 mM dithiothreitol [DTT], 0.03% bromophenol blue) were added to each fraction, and samples were boiled for 3 min and then subjected to SDS-PAGE and Western blot analysis.

TABLE 1 Plasmids used in this study

Plasmid	Description[a]	Construction[b]	Reference or source
pZR12	Kan^r; T7-pro-σ^K(1–126)-H6		68
pZR173	Kan^r; T7-σ^K(21–126)-H6	pZR12 was subjected to SDM with primers LK1567 and LK1568 to delete first 20 residues of pro-σ^K	This study
pZR200	Amp^r; T7-F2-H6 cloning vector		67
pZR209	Amp^r; T7-cytTM-SpoIVFB-F2-H6		67
pZR327	Kan^r; T7-pro-σ^K(1–126)-S20G-H6		67
pZR615	Amp^r Kan^r; Ava_1070	ava_1070 amplified with primers ZR07 and ZR08, cloned into pCR2.1-TOPO	This study
pZR616	Amp^r Kan^r; Ava_1730	ava_1730 amplified with primers ZR09 and ZR10, cloned into pCR2.1-TOPO	This study
pZR617	Amp^r Kan^r; Ava_3438	ava_3438 amplified with primers ZR11 and ZR12, cloned into pCR2.1-TOPO	This study
pZR618	Amp^r; T7-MCS-F2-H6	pZR200 was subjected to SDM with primers ZR05 and ZR06 to create SacI and NheI sites downstream of F2-H6	This study
pZR661	Amp^r Kan^r; Ava_4785	ava_4785 amplified with primers ZR13 and ZR14, cloned into pCR2.1-TOPO	This study
pZR662	Amp^r Kan^r; Ava_1797	ava_1797 amplified with primers ZR03 and ZR04, cloned into pCR2.1-TOPO	This study
pZR632	Amp^r; T7-Ava_1730-F2-H6	NdeI-SalI fragment excised from pZR616, subcloned into NdeI-SalI-digested pZR618	This study
pZR633	Amp^r; T7-Ava_3438-F2-H6	NdeI-SalI fragment excised from pZR617, subcloned into NdeI-SalI-digested pZR618	This study
pZR634	Amp^r; T7-Ava_1070-H6	BamHI-SalI fragment excised from pZR615, subcloned into BamHI-XhoI-digested pZR209	This study
pZR796	Amp^r ; T7-cytTM-Ava_1797-F2-H6	BamHI-HindIII fragment excised from pZR662, subcloned into BamHI-HindIII-digested pZR209	This study
pZR797	Amp^r; T7-Ava_4785-F2-H6	NcoI-HindIII fragment excised from pZR661, subcloned into NcoI-HindIII-digested pZR209	This study
pZR817	Amp^r; T7-cytTM-Ava_1797(E63Q)-F2-H6	pZR796 was subjected to SDM with primers ZR144 and ZR145 to make an E63Q mutation	This study
pZR819	Amp^r; T7-Ava_4785(E67Q)-F2-H6	pZR797 was subjected to SDM with primers ZR146 and ZR147 to make an E67Q mutation	This study
pZR820	Amp^r; T7-Ava_1730(E18Q)-F2-H6	pZR632 was subjected to SDM with primers ZR142 and ZR143 to make an E18Q mutation	This study
pZR827	Amp^r; T7-cytTM-MCS-F2-H6	Oligonucleotides ZR161 and ZR167 were annealed, forming a MCS, which was cloned into BamHI-HindIII-digested pZR209	This study
pZR830	Amp^{r}Kan^r; Ava_1070(201–417)	ava_1070(201–417) amplified with primers ZR216 and ZR218, cloned into pCR2.1-TOPO	This study
pZR844	Amp^{r}Kan^r; Ava_3438(184–407)	ava_3438(184–407) amplified with primers ZR214 and ZR215, cloned into pCR2.1-TOPO	This study
pZR845	Amp^r; T7-cytTM-Ava_3438(184–407)-F2-H6	NdeI-SalI fragment excised from pZR844, subcloned into NdeI-SalI-digested pZR827	This study
pZR874	Amp^r; T7-cytTM-Ava_1070(201–417)-F2-H6	NdeI-SalI fragment excised from pZR830, subcloned into NdeI-SalI-digested pZR827	This study
pZR922	Amp^r; T7-cytTM-Ava_1070(201–417)E266Q-F2-H6	pZR874 was subjected to SDM with primers ZR170 and ZR171 to make an E266Q mutation	This study
pZR940	Amp^r; T7-cytTM-Ava_3438 (184–407)E259Q-F2-H6	pZR845 was subjected to SDM with primers ZR168 and ZR169 to make an E259Q mutation	This study

[a] Amp^r, ampicillin; Kan^r, kanamycin; T7, T7 RNA polymerase promoter and a translation initiation sequence; F2, two FLAG epitopes; H6, six histidine residues; cytTM, transmembrane segment from rabbit cytochrome P450 2B4 (67); MCS, multiple cloning site.
[b] Unless stated otherwise, the template for PCRs was *A. variabilis* genomic DNA. SDM, site-directed mutagenesis.

Western blot analysis. Equivalent amounts of *E. coli* cells (depending on the optical density at 600 nm) were collected from 0.5 to 1.0 ml of culture by centrifugation (12,000 × *g*). Whole-cell extracts were prepared as described previously (68) with the exception of the two coexpression samples of truncated Ava_1070(201–417) and Ava_3438(184–407) plus pro-σ^K(1–126)S20G. These two coexpression samples were resuspended as above in PBS lysis buffer and incubated at 37°C for 10 min and then subjected to sonication under 25% amplitude (three times for 10 s with a 5-s interval in an ice-water bath) (Digital Sonifer; Branson), and cell debris was separated by centrifugation at 12,000 × *g* for 10 min. The proteins in the low-speed supernatant were separated by SDS-PAGE and subjected to Western blot analysis as described previously (32). Antibodies against pentahistidine (Qiagen) and FLAG (Sigma) were used at 1:5,000 dilutions.

Purification of proteins. *E. coli* cells (100 ml) bearing pZR327 [pro-σ^K(1–126)S20G-H6, where H6 indicates a His_6 tag] alone or in combination with pZR209 (cytTM-SpoIVFB-F2-H6, where F2 indicates two copies of a FLAG tag), pZR796 [cytTM-Ava_1797-F2-H6], pZR797

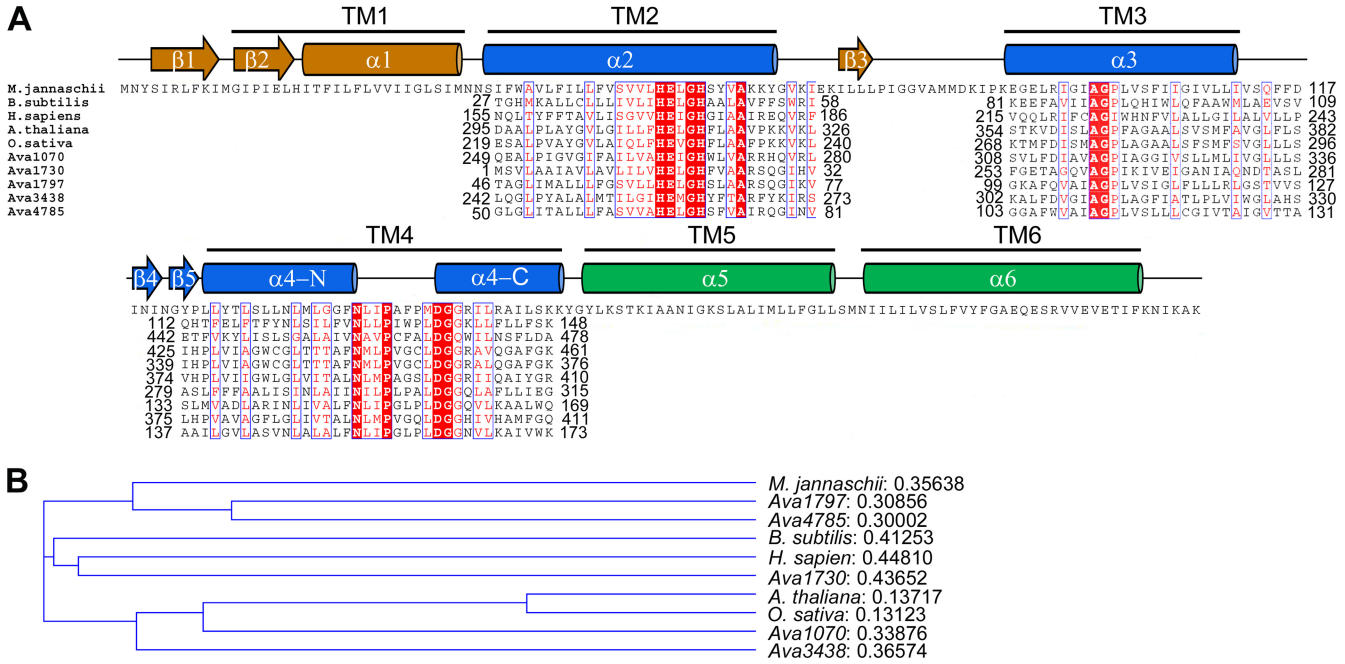

FIG 2 Sequence alignment and phylogenetic tree of five putative *A. variabilis* site-2 proteases. (A) Sequence alignment of five S2Ps$_{Av}$ with other homologs in diverse species including higher plants and humans. Secondary structural elements of S2P$_{Mj}$, a site-2 protease (S2P) from *M. jannaschii* (17), are shown at the top of the alignment. Three highly conserved motifs, HEXXH, AG(P/I), and N(X)$_7$DG, are highlighted in red. The aligned sequences are *M. jannaschii* (GI 2499926), *B. subtilis* (GI 16079849), *H. sapiens* (GI 6016601); *A. thaliana* (GI 15238440), *O. sativa* (GI Os03g0792400), and *A. variabilis* (Ava_1070, Ava_1730, Ava_1797, Ava_3438, and Ava_4785). (B) Phylogenetic tree of five putative S2Ps$_{Av}$ and the other five homologs in bacteria, archaea, higher plants, and human. The five S2Ps$_{Av}$ are branched into three groups: Ava_1797 and Ava_4785 are close to archaeal *M. jannaschii* S2P; Ava_1070 and Ava_3438 are close to proteins of higher plants (*A. thaliana* and *O. sativa*); Ava_1730 is close to proteins of human and bacteria (*H. sapiens* and *B. subtilis*).

(Ava_4785-F2-H6), and pZR817 [cytTM-Ava_1797(E63Q)-F2-H6] were harvested by centrifugation at 12,000 × *g* for 10 min at 4°C. The pellets were resuspended in 12 ml of PBS lysis buffer, disrupted by passage through a Nano DeBEE electric benchtop laboratory homogenizer, and subjected to ultracentrifugation. Cytoplasmic fraction used for purification of σ^K(21-126)-H6 and membrane fraction used for purification of pro-σ^K(1-126)S20G-H6 were prepared as described above. Talon Superflow Resin (Clontech) was used to purify σ^K(21-126)-H6 and pro-σ^K(1-126)S20G-H6 following the manufacturer's instructions. Amicon Ultra-4 Centrifugal Filter Units with a 10-kDa cutoff (Millipore) were used to concentrate samples. Purified and concentrated samples were subjected to quadrupole time of flight (Q-TOF) mass spectrometry (MS) and SDS-PAGE, followed by Coomassie blue R-250 staining and Western blot analysis.

N-terminal sequencing. *E. coli* cells bearing pZR327 [pro-σ^K(1–126)S20G-H6] in combination with pZR797 were induced and harvested as described above in 100 ml of LB broth with appropriate antibiotics. Unprocessed pro-σ^K(1–126)S20G-H6 and the processed product were purified from the low-speed supernatant (12,000 × *g*) using Talon Superflow Resin (Clontech) following the manufacturer's instructions. The purified processed and unprocessed proteins were separated on 14% SDS-PAGE with Tris-Tricine buffer (0.1 M Tris, 0.1 M Tricine, and 0.1% SDS), electroblotted onto Sequi-Blot polyvinylidene difluoride (PVDF) membrane (Bio-Rad), stained with Coomassie solution (0.1% Coomassie brilliant blue R-250, 1% acetic acid, and 40% methanol), and destained with 50% methanol. The faster-migrating processed protein was submitted to the Michigan State University Macromolecular Structure Facility for N-terminal sequencing.

Mass spectrometry. Mass spectrometric analysis was performed at the South Dakota Biomedical Research Infrastructure Network (SD BRIN) Proteomics Core Facility (University of South Dakota). The purified proteins were desalted using ZipTip with 0.6 μl of C_{18} resin (Millipore). Then proteins were diluted two times in water-acetonitrile-trifluoroacetic acid (TFA) (49.9:50:0.1) and 1 to 2 μl (approximately 25 ng/μl) was injected into the quadrupole time of flight mass spectrometer using a syringe pump (Q-TOF Micro; Waters Micromass). The ionization was performed in positive mode through a nanoelectrospray ionization (nano-ESI) probe in MS mode with the following parameters: capillary voltage, 3,500 V; sample cone, 35 V; and extraction cone, 2.0 V. The ESI spectra with multiple charge states were acquired using MassLynx software, version 4.1 (Waters Micromass), at an *m/z* range of 600 to 2,500 Da and deconvoluted using the MaxEnt1 tool of MassLynx, version 4.1, with the following parameters: range, 12,500 to 16,000 Da; resolution, 0.5 Da/channel. The instrument was calibrated using 100 ng/μl myoglobin from horse (Sigma-Aldrich) before the samples were run.

RESULTS

Identification of five putative site-2 protease genes in the *A. variabilis* genome. Genome-wide comparative analysis of S2P metalloproteases in *A. variabilis* identified five genes (ava_1070, ava_1730, ava_1797, ava_3438, and ava_4785) encoding homologues of the S2P family using SpoIVFB from *B. subtilis* as a template. As shown in Fig. 2A, Ava_1070, Ava_1730, Ava_1797, Ava_3438, and Ava_4785 all contain three conserved motifs, HEXXH, AG(P/I), and N(X)$_7$DG, typical signatures of the S2P metalloprotease family. Although the core domains (α-helices 2, 3, and 4) of S2Ps are highly conserved from bacteria to humans, the primary sequences and distribution of core domains are very diverse. Only the core domains can be aligned, and sequence homology elsewhere is negligible. The five S2Ps$_{Av}$ are branched into three groups: Ava_1797 and Ava_4785 are close to the archaeon *Methanocaldococcus jannaschii* S2P (S2P$_{Mj}$), Ava_1070 and

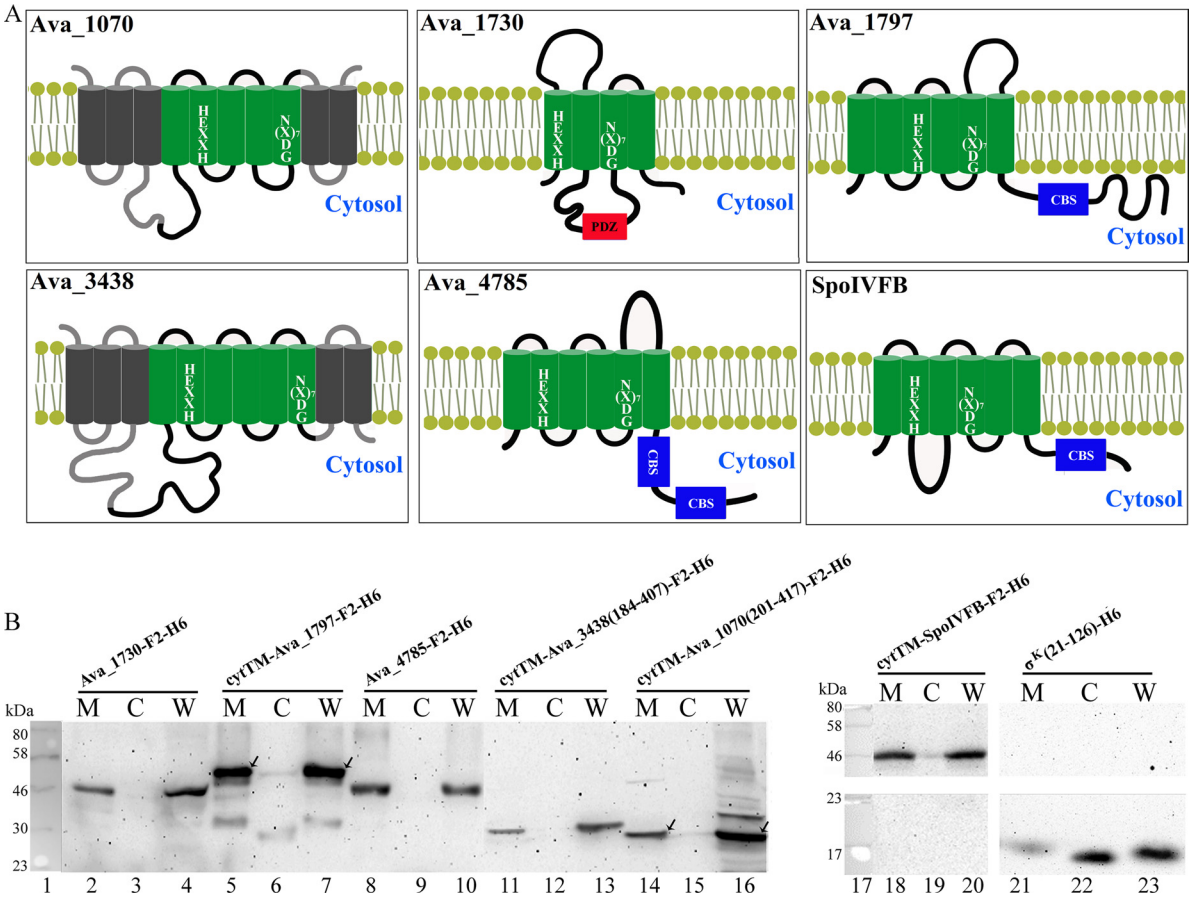

FIG 3 Five S2Ps$_{Av}$ are membrane proteins. (A) Schematic representation of the predicted topology of five S2Ps$_{Av}$ and SpoIVFB. Putative transmembrane helices were predicted using TMHMM (30). The length of the line is proportional to its amino acid sequence length. The C-terminal cystathionine-β-synthase (CBS) domain and PDZ domain are highlighted in blue and red, respectively. Ava_1070(201–417) and Ava_3438(184–407) are truncated versions of full-length proteins without the portions shown in gray. (B) Five S2Ps$_{Av}$ were detected in the membrane fraction. *E. coli* cells bearing pZR632 to produce Ava_1730-F2-H6 (43 kDa; lanes 2 to 4), pZR796 to produce cytTM-Ava_1797-F2-H6 (50 kDa; lanes 5 to 7), pZR797 to produce Ava_4785-F2-H6 (43 kDa; lanes 8 to 10), pZR845 to produce truncated cytTM-Ava_3438(184–407)-F2-H6 (31 kDa; lanes 11 to 13), pZR874 to produce truncated cytTM-Ava_1070(201–417)-F2-H6 (31 kDa; lanes 14 to 16), pZR209 to produce cytTM-SpoIVFB-F2-H6 (42 kDa; lanes 18 to 20) as a control for membrane protein, and pZR173 to produce σ^K(21–126)-H6 (13 kDa; lanes 21 to 23) as a control for cytoplasmic protein were collected 3 h after IPTG induction. Extracts from equivalent cell amounts were fractionated as whole-cell lysate (W), the low-speed (12,000 × *g*) supernatant from centrifugation, the cytoplasmic fraction (C), and membrane fraction (M) after ultracentrifugation (200,000 × *g*) and then immunoblotted using antibodies against FLAG (left and top right panels) or His$_6$ tag (bottom right panel).

Ava_3438 are close to S2Ps of higher plants (*Arabidopsis thaliana* and *Oryza sativa*), and Ava_1730 is close to S2Ps of human and bacteria (*H. sapiens* and *B. subtilis*) (Fig. 2B), implying that they may be involved in various signaling functions and have distinct substrate specificities.

In addition to the core domains, C-terminal cystathionine-β-synthase (CBS) domains, which can bind adenosine-containing ligands such as ATP, AMP, or *S*-adenosylmethionine (25), are found in Ava_1797 and Ava_4785 (Fig. 3A). Previous studies suggested that the CBS domain of SpoIVFB interacts with its substrate pro-σ^K and that ATP influences their interaction in *B. subtilis* (67), suggesting that Ava_1797 and Ava_4785 might have a substrate similar to pro-σ^K in *A. variabilis*. A PDZ domain, a small protein module that promotes protein-protein interactions through association with other protein domains in their partner proteins to carry out their specific functions, is found in Ava_1730 (Fig. 3A). It has been demonstrated that the PDZ domain of SpoIVB is responsible for protein interactions in the process of activation of the σ^K in *B. subtilis* (13).

Five putative S2Ps$_{Av}$ are transmembrane proteins. Putative transmembrane helices (TMHs) in five S2Ps$_{Av}$ were predicted using TMHMM (30) through the web server available at http://www.cbs.dtu.dk/services/TMHMM/. As seen in Fig. 3A, the total number of transmembrane helices in S2Ps$_{Av}$ range from 4 in Ava_1730 to 11 in Ava_3438, even though all five S2Ps$_{Av}$ consist of HEXXH and N(X)$_7$DG motifs in their core domain TMHs. To determine whether these putative S2Ps$_{Av}$ are indeed membrane proteins, individual full-length S2Ps$_{Av}$ fused to C-terminal tandem tags consisting of two copies of the FLAG tag (F2) and His$_6$ (H6) were overexpressed in *E. coli* and subjected to subcellular fractionation. Total proteins from the resulting whole-cell lysate and cytoplasmic and membrane fractions were separated by SDS-PAGE and subjected to Western blotting using anti-FLAG antibody to monitor S2Ps. As shown in Fig. 3B, Ava_1730 and Ava_4785 were expressed (lanes 4 and 10, respectively) and present exclusively in the membrane fraction (lanes 2 and 8, respectively). However, the expression of full-length Ava_1797, Ava_3438, and Ava_1070, which are predicted to have 6, 11, and 10 transmembrane seg-

ments, respectively, was not detectable (data not shown) in whole-cell lysates, probably due to their poor expression. Because the $S2P_{Av}$ expression levels were below the limits of detection in this experiment, an attempt to increase $S2P_{Av}$ expression was made by fusing a transmembrane segment (denoted cytTM, residues 1 to 23) from rabbit cytochrome P450 2B4 to the 5′ end of each $S2P_{Av}$ gene. This cytTM had been successfully used to improve the expression of SpoIVFB when fused to its N terminus (67). As shown in Fig. 3B, cytTM-Ava_1797-F2-H6 was detectable (lane 7) and present solely in the membrane fraction (lane 5); however, cytTM-Ava_1070-F2-H6 and cytTM-Ava_3438-F2-H6 were still below their detection limits (data not shown). Since a truncated $S2P_{Mj}$ containing all the core domains accumulated well in *E. coli* and maintained proteolytic activity (17), it is possible to improve Ava_1070 and Ava_3438 expression levels in *E. coli* through elimination of some transmembrane helices. To this end, TMHs 1 to 3 and 9 to 10 of Ava_1070 (Fig. 3A) and TMHs 1 to 3 and 10 to 11 of Ava_3438 (Fig. 3A) were deleted. As seen in Fig. 3B, the truncated proteins cytTM-Ava_3438(184–407)-F2-H6 and cytTM-Ava_1070(201–417)-F2-H6 were expressed (lanes 13 and 16, respectively) and present solely in the membrane fraction (lanes 11 and 14, respectively). Taking these results together, we conclude that all five $S2Ps_{Av}$ are membrane proteins.

The five putative $S2Ps_{Av}$ are capable of cleaving *Bacillus* pro-σ^K in a reconstituted *E. coli* system. Unlike the conventional proteolytic enzymes, polytopic I-CLips with catalytic-site motifs embedded within transmembrane segments (2, 17, 19, 58) cleave the transmembrane helix of substrates inside the lipid bilayer. It is very difficult to purify such membrane enzymes and reconstitute their activities *in vitro*. To circumvent this problem, we previously established an *E. coli* system for studying *Bacillus* RIP and demonstrated that SpoIVFB specifically cleaves the N-terminal membrane segment of an MTF pro-σ^K, releasing active σ^K from the *E. coli* cytoplasm membrane into the cytosol (68, 69). Before a physiological substrate is identified, certain transmembrane proteins can serve as artificial substrates to test the proteolytic activities of site-2 proteases (2, 17). Using the reconstituted *E. coli* system with pro-σ^K as an artificial substrate, we tested the hypothesis that the five $S2Ps_{Av}$ have intramembrane proteolytic activities. First, five putative $S2P_{Av}$ genes (ava_1070, ava_1730, ava_1797, ava_3438, and ava_4785) were individually cloned into pZR200 (a pET21b-derived expression vector C-terminally tagged with two copies of a FLAG tag and His_6 in tandem; Amp^r). Next, each of these five plasmids was cotransformed with pZR327 [for expression of *Bacillus* pro-σ^K(1–126)S20G-H6 in *E. coli*; Kan^r] into BL21(DE3) to test the specific proteolytic cleavage of pro-σ^K(1–126)S20G-H6 by each putative $S2P_{Av}$. Pro-σ^K(1–126)S20G-H6 (67) was cleaved by SpoIVFB more efficiently than the wild-type pro-σ^K(1–126)-H6. So, the mutant pro-σ^K(1–126)S20G-H6 was selected to test the proteolytic activity of the five $S2Ps_{Av}$. As shown in Fig. 4A and in Fig. S1 in the supplemental material, three putative S2Ps (Ava_1730, Ava_3438, and Ava_1070) were capable of cleaving pro-σ^K(1–126)S20G-H6. The cleavage products (Fig. 4A, lanes 4, 7, and 8, respectively) nearly comigrated with σ^K(21–126)-H6 (lane 5) but were not detected in control samples (lanes 2, 3, 6, and 9, respectively), indicating that Ava _1730, Ava_3438, and Ava_1070 have intramembrane cleaving protease activity for pro-σ^K(1–126)S20G-H6. Because some $S2P_{Av}$ expression levels were below the detection limit in this experiment, an attempt to increase $S2P_{Av}$ expression was made by either fusing a cytTM to the 5′ end of each $S2P_{Av}$ gene or eliminating some transmembrane helices outside the S2P core domains (Fig. 3A and B). As expected, Ava_1730, Ava_4785, Ava_1797, truncated Ava_3438(184–407), and truncated Ava_1070(201–417) were capable of cleaving pro-σ^K(1–126)S20G-H6 (Fig. 4B, lanes 2, 4, 6, 10, and 12, respectively). The cleavage products nearly comigrated with σ^K(21–126)-H6 (lane 8). We conclude that Ava_1730, Ava_4785, Ava_1797, Ava_3438, truncated Ava_3438(184–407), Ava_1070, and truncated Ava_1070(201–417) have intramembrane-cleaving protease activity.

Bioinformatic analysis of five putative $S2Ps_{Av}$ showed that they all contain three motifs, HEXXH, AG(P/I), and $N(X)_7DG$, which are strictly conserved in S2P metalloproteases. It is known that a catalytic glutamic acid (E) and two metal-coordinating histidines (H) in the HEXXH motif and a third metal-coordinating aspartic acid (D) in the $N(X)_7DG$ motif together form a zinc-binding site, which is the catalytic center of the S2Ps (38). It is thought that the glutamic acid activates a water molecule for cleaving an extended and therefore accessible TMH substrate peptide bond (48). If these five putative $S2Ps_{Av}$ are metalloproteases, then changing the glutamic acid residue to glutamine (Q) will prevent metal binding and cause reduction or even loss of proteolytic activity. To address the hypothesis that the five $S2Ps_{Av}$ are zinc metalloproteases, the effect of $S2P_{Av}^{E\rightarrow Q}$ mutants in the HEXXH motif was investigated. As shown in Fig. 4C, all five $S2P_{Av}^{E\rightarrow Q}$ mutants failed to cleave pro-σ^K(1–126)S20G-H6, suggesting that the proteolytic activities of the five $S2Ps_{Av}$ were abolished by changing E to Q in the HEXXH motif. Thus, our results provide further evidence that these five putative $S2Ps_{Av}$ are metalloproteases.

Ava_4785 and Ava_1797 accurately cleaved pro-σ^K(1–126)S20G-H6. To determine where the $S2Ps_{Av}$ cleave pro-σ^K(1–126)S20G-H6, N-terminal sequencing and mass spectrometry techniques were used in this study. N-terminal sequencing was conducted to determine the N-terminal amino acid sequence of the cleavage product by Ava_4785, which had the strongest band based on Coomassie staining among the five $S2Ps_{Av}$ (Fig. 5F, lane 8). The determined N-terminal sequence of the peptide cleaved by Ava_4785 is YVKNN (see Fig. S2 in the supplemental material), which is identical to that of σ^K(21–126)-H6 cleaved by SpoIVFB from *B. subtilis*. Furthermore, the purified products of pro-σ^K(1–126)S20G-H6 cleaved by Ava_4785 and Ava_1797 (Fig. 5F, lanes 8 and 9, respectively) were also analyzed by quadrupole time of flight (Q-TOF) mass spectrometry. As positive controls, intact pro-σ^K(1–126)S20G-H6 (Fig. 5F, lane 12) and the peptide σ^K(1–126)S20G-H6 cleaved by cytMT-SpoIVFB-F2-H6 (Fig. 5F, lane 10) were also analyzed. Q-TOF MS detected peaks at 15,035.3 Da (Fig. 5E) and 12,852 Da (Fig. 5C), respectively, which are in good agreement with their calculated masses of 15,031 Da for pro-σ^K(1–126)S20G-H6 and 12,853 Da for σ^K(21–126)-H6. The mass of the peptide cleaved by Ava_4785 (Fig. 5A) or Ava_1797 (Fig. 5B) was 12,851.5 Da, which matched very well with the theoretical mass of σ^K(21–126)-H6 (12,853 Da). In addition, no signals were observed around 12,853 Da from the purified materials through Talon Superflow Resin from cultures coexpressing Ava_1797(E63Q)-F2-H6/Pro-σ^K(1–126)S20G-H6 by Q-TOF MS (Fig. 5D), Coomassie staining (Fig. 5F, lane 11), and Western blotting (Fig. 5F, lane 5), further confirming that the 12,851.5-Da peaks detected from Ava_4785 and Ava_1797 are σ^K(21–126)-H6. Therefore, we conclude that $S2Ps_{Av}$ (Ava_4785 and Ava_1797) cleave the same glycine-tyrosine bond (Fig. 5G) in pro-σ^K(1–126)S20G-H6 as is cleaved by SpoIVFB (67).

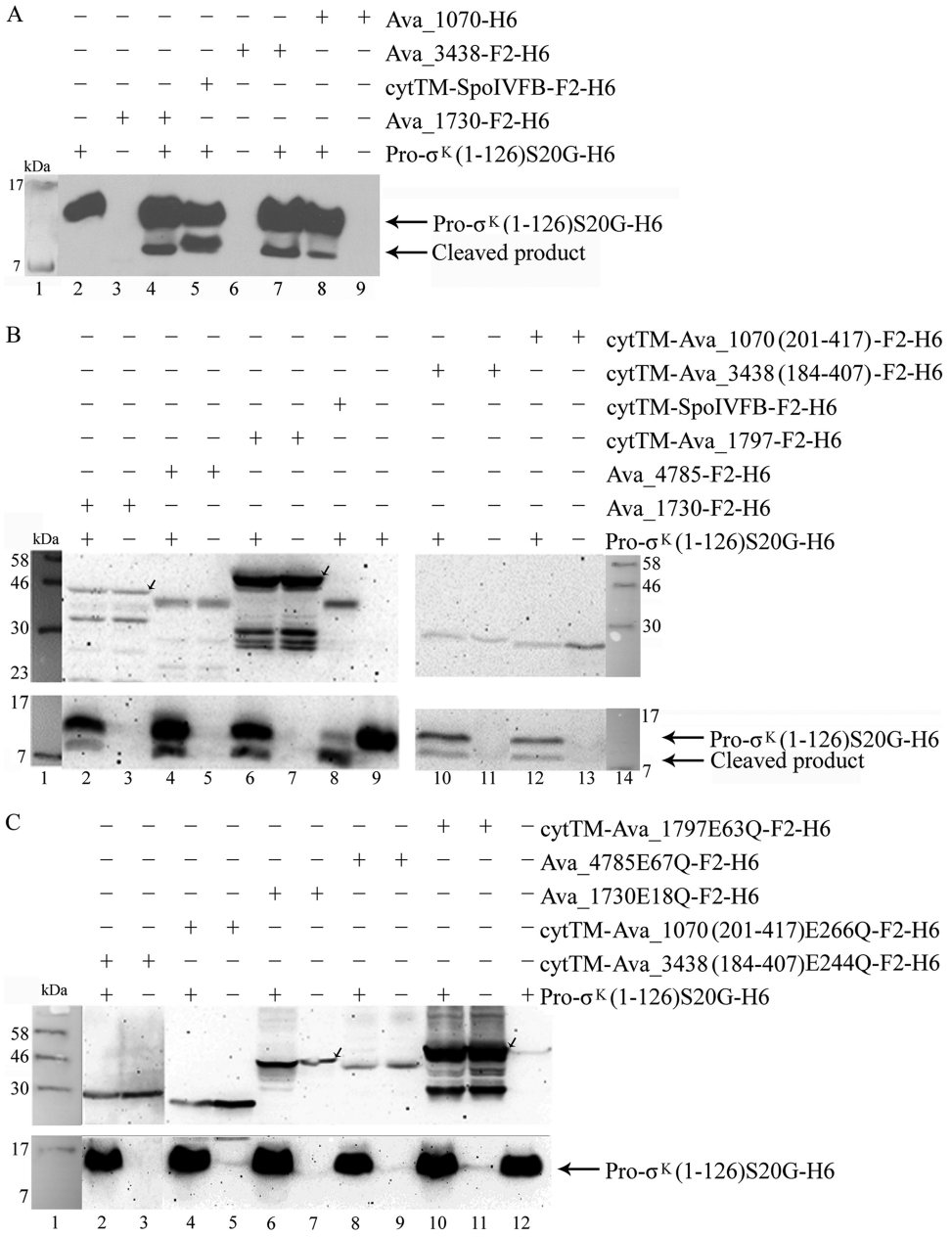

FIG 4 Five S2Ps$_{Av}$ are site-2 metalloproteases. (A) Proteolytic activities of full-length Ava_1070, Ava_1730, and Ava_3438. *E. coli* cells bearing pZR632 (Ava_1730-F2-H6) (lane 3) or pZR633 (Ava_3438-F2-H6) (lane 6), pZR634 (Ava_1070-H6) (lane 9) alone or in combination with pZR327 [pro-σ^K(1–126)S20G-H6] (lanes 4, 7, and 8, respectively) were induced with IPTG for 3 h to express the indicated proteins; then whole-cell extracts were subjected to Western blot analysis using antibodies against pentahistidine. *E. coli* cells bearing pZR327 [pro-σ^K(1–126)S20G-H6] alone (lane 2) or in combination with pZR209 (cytTM-SpoIVFB-F2-H6) (lane 5) serve as negative and positive controls. (B) Proteolytic activities of five S2Ps$_{Av}$. *E. coli* cells bearing pZR632 (Ava_1730-F2-H6) (lane 3), pZR797 (Ava_4785-F2-H6) (lane 5), pZR796 (cytTM-Ava_1797-F2-H6) (lane 7), pZR845 [cytTM-Ava_3438(184–407)-F2-H6] (lane 11), or pZR874 [cytTM-Ava_1070(201–417)-F2-H6] (lane 13) alone or in combination with pZR327 [pro-σ^K(1–126)S20G-H6] (lanes 2, 4, 6, 10, and 12, respectively) were induced with IPTG for 3 h to express the indicated proteins; then whole-cell extracts were subjected to Western blot analysis using antibodies against FLAG (top panels) or pentahistidine (bottom panels). *E. coli* cells bearing pZR327 [pro-σ^K(1–126)S20G-H6] alone (lane 9) or in combination with pZR209 (cytTM-SpoIVFB-F2-H6) (lane 8) serve as negative and positive controls. (C) Proteolytic activities of the five S2Ps$_{Av}$ were abolished by the E-to-Q substitution in the HEXXH motif, a hallmark of S2P metalloproteases. *E. coli* cells bearing pZR940 [cytTM-Ava_3438(184–407)E244Q-F2-H6] (lane 3), pZR922 [cytTM-Ava_1070(201–417)E266Q-F2-H6] (lane 5), pZR820 [Ava_1730(E18Q)-F2-H6] (lane 7), pZR819 [Ava_4785(E67Q)-F2-H6] (lane 9), or pZR817 [cytTM-Ava_1797(E63Q)-F2-H6] (lane 11) alone or in combination with pZR327 [pro-σ^K(1–126)S20G-H6] (lanes 2, 4, 6, 8, 10, respectively) were induced with IPTG for 3 h to express the indicated proteins; then whole-cell extracts were subjected to Western blot analysis using antibodies against FLAG (top panel) or pentahistidine (bottom panel). *E. coli* cells bearing pZR327 [pro-σ^K(1–126)S20G-H6] alone (lane 12) serve as a negative control.

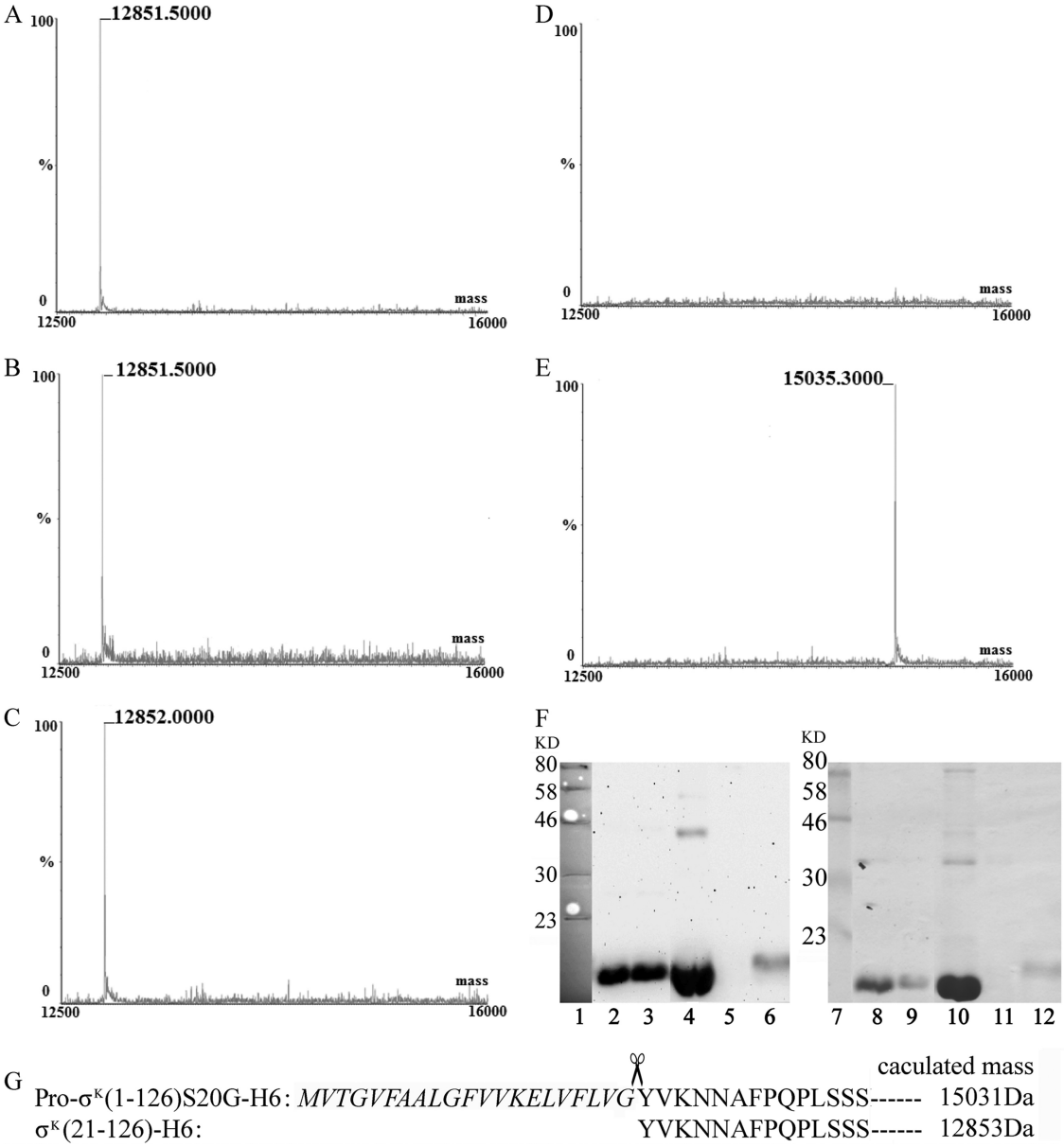

FIG 5 Mass spectrometric analysis for the peptides cleaved by $S2Ps_{Av}$. Q-TOF mass identification of peptides cleaved by Ava_4785-F2-H6 (A), cytTM-Ava_1797-F2-H6 (B), cytTM-SpoIVFB-F2-H6 (C), or cytTM-Ava_1797(E63Q)-F2-H6 (D) is shown. As a control, the *m/z* spectrum of intact pro-σ^K(1–126)S20G-H6 is also shown (E). (F) Purified pro-σ^K(1–126(S20G)-H6 or σ^K(21–126)-H6 detected by Coomassie staining (right panel) and Western blotting (left panel). Lanes 2 and 8, purified σ^K(21–126)-H6 cleaved by Ava_4785-F2-H6; lanes 3 and 9, purified peptide-H6 cleaved by cytTM-Ava_1797-F2-H6; lanes 4 and 10, purified peptide-H6 cleaved by cytTM-SpoIVFB-F2-H6; lanes 5 and 11, purified sample from cytTM-Ava_1797(E63Q)-F2-H6; lanes 6 and 12, purified pro-σ^K(1–126)S20G-H6. The calculated masses of σ^K(21–126)-H6 and pro-σ^K(21–126)S20G-H6 are 12,853 Da and 15,031 Da, respectively. (G) Partial amino acid sequence of pro-σ^K(1–126)S20G-H6 and σ^K(21–126)-H6. The cleavage site was mapped between residues Gly^{20} and Tyr^{21} by SpoIVFB. The italicized sequences represent transmembrane helix of pro-σ^K(1–126)S20G-H6.

DISCUSSION

RIP is a newly discovered but little understood mechanism that controls many important signaling pathways conserved from bacteria to human. In this report, five putative site-2-type I-CLips were initially identified in *A. variabilis* by a genome-wide bioinformatics analysis. We tested proteolytic activities of five putative $S2Ps_{Av}$ toward pro-σ^K(1–126)S20G-H6 and showed that all five S2Ps are capable of cleaving pro-σ^K(1–126)S20G-H6. Further analyses by N-terminal sequencing and Q-TOF mass spectrometry revealed that $S2Ps_{Av}$ accurately cleave the same glycine-tyrosine bond in pro-σ^K(1–126)S20G-H6 as is cleaved by the cognate enzyme SpoIVFB. Furthermore, we showed, for the first time, that the five $S2Ps_{Av}$ display HEXXH-dependent catalytic activities.

Substrate specificity of S2P type I-CLips. Both Ava_4785 and Ava_1797 contain the CBS domains found in SpoIVFB and exhibit the highest proteolytic activities (40 to 44%) toward pro-σ^K, while the cognate protease SpoIVFB showed 64% cleavage efficiency in *E. coli* (see Fig. S3 in the supplemental

material). The other three $S2Ps_{Av}$ (Ava_1730, truncated Ava_1070, and truncated Ava_3438) without CBS domains also showed lower proteolytic activities (30 to 33%) (see Fig. S3) toward pro-σ^K. Ava_1070, perhaps because it had the poorest expression in *E. coli*, showed much lower proteolytic activity (see Fig. S1, lanes 10 to 12, in the supplemental material) than its truncated version (Fig. 4B, lane 12).

In summary, all five $S2Ps_{Av}$, including the truncated ones, are capable of cleaving the artificial substrate MTF pro-σ^K to some extent (Fig. 4A and B; see also Fig. S3 in the supplemental material). The apparent nonspecificity of the five $S2Ps_{Av}$ here raises the question of their biological significance. There is some evidence that S2Ps can cleave multiple substrates; e.g., human S2P cleaves both SREBP and ATF6 (65), and YluC (a *Bacillus* S2P) cleaves both RsiW (50) and FtsL (6) in *B. subtilis*. We anticipate that other cofactors/associated proteins in the biological systems may be involved in S2P specificity determination. Moreover, the RIP signaling pathways can also be regulated temporally and spatially by controlling gene expression levels and their subcellular localizations, which may further contribute to S2P substrate specificity. Although the physiological substrates for these five $S2Ps_{Av}$ are currently unknown, the 14 putative genes encoding MTFs identified (data not shown) in the genome of *A. variabilis* are being tested for substrate possibility.

Overexpression of functional I-CLips in *E. coli*. An attempt to overexpress the full-length $S2Ps_{Av}$ in *E. coli* was made to study their subcellular localization and enzymatic activities. Three proteins (Ava_1730, Ava_1797, and Ava_4785) are detectable, while the other two (Ava_1070 and Ava_3438) are not, possibly due to complex topological properties. Ten TMHs and 11 TMHs (Fig. 3A) were predicted in Ava_1070 and Ava_3438, respectively, by the transmembrane prediction program TMHMM. To solve this problem, truncated versions of Ava_1070 and Ava_3438 were created with their core domains kept intact. As expected, the expression levels of truncated Ava_1070(201-417) and Ava_3438(184-407) became detectable (Fig. 3B). To confirm that these five proteins were transmembrane metalloproteases, we fractionated the whole-cell lysate into cytoplasmic and membrane fractions, which revealed that all five $S2P_{Av}$ (three full-length and two truncated) proteins were present solely in the membrane fraction. Furthermore, we showed, for the first time, that five $S2Ps_{Av}$ display HEXXH-dependent catalytic activities, which categorize these five $S2Ps_{Av}$ as a family of intramembrane metalloproteases.

Addition of cytTM to the N terminus of SpoIVFB (a *Bacillus* I-CLip) increased its accumulation in *E. coli* by at least 100-fold (67). The same approach was successful in increasing the yield of Ava_1797 (Fig. 4B, lanes 6 and 7). On a per cell base, cytTM-Ava_1797 accumulation in *E. coli* was about three times higher (Fig. 4B and data not shown) than that of cytTM-SpoIVFB. The higher level of expression for Ava_1797 indicates that it will be possible to do deeper biochemical and structural analyses for this group of I-CLips.

Over 1,857 putative S2Ps were identified in 1,426 available genomes (http://merops.sanger.ac.uk/cgi-bin/make_frame_file?id=M50); however, it is more difficult to study RIP events in higher plants and human due to their more complex organismal nature and the lack of powerful genetic tools. Only a few S2P-type proteases have been studied to date due to lack of an efficient experimental system to study such a polytopic intramembrane metalloprotease (2, 3, 8, 10, 67). Our reconstituted *E. coli* system in which a putative S2P is coexpressed with an artificial substrate should be applicable to studies of other RIP events and adaptable to the characterization of I-CLips from all life forms.

S2Ps may mainly be involved in stress response and stress-induced cellular differentiation. RIP is a conserved process, and the proteases involved are evolutionarily related. In 1,426 available genomes, about 70% have one or more putative S2Ps. Interestingly, all five putative $S2Ps_{Av}$ are found to have orthologs in 10 out of 39 cyanobacterial genomes (http://genome.kazusa.or.jp/cyanobase), with the exception of *Nostoc punctiforme*, which has one more S2P, Npun_R1354 (see Table S2 in the supplemental material). One to four putative S2Ps were found in 29 other cyanobacterial genomes (see Table S2). Furthermore, six putative S2Ps were also found in the genomes of *Arabidopsis thaliana* (see Table S2). Unlike cyanobacteria and higher plants, animals tend to have fewer putative S2Ps in their genomes, despite their complexities. Surprisingly, in 85 completed animal genomes, there is only one putative S2P found in each of the 62 mammal genomes and none in the other 23 genomes. Perhaps this discrepancy reflects an evolutionary adaptation because animals can "escape" a harsh environmental condition and therefore encounter fewer stresses, while plants and many microorganisms have to evolve adaptive mechanisms for survival under stress conditions from which they cannot move away. Consistent with this hypothesis, microarray data strongly suggest that S2Ps play important roles in the numerous stress responses of *Arabidopsis* (Genevestigator database; Nebion AG, Zurich Switzerland) (see Table S2). In addition to the correlation with stress responses, the distribution of S2P genes in prokaryotic genomes appears to be well correlated with the complexity of cellular differentiation. For example, *E. coli*, with no cellular differentiation, has only one S2P, *B. subtilis*, with spore formation, has four S2Ps, *Myxococcus xanthus*, with complex fruiting body formation, also has five putative S2Ps, while *A. variabilis* with four types of differentiated cells has five putative S2Ps. Based on this survey, some microarray data (9, 14), and high-throughput sequencing of RNA transcripts (RNA-seq) (18), we speculate that S2Ps in *A. variabilis* may be primarily involved in stress responses, including the regulation of stress-induced cellular differentiation that seldom or never occurs in animals. With our preliminary results indicating that Ava_4785 is involved in the cold response and that Ava_1730 also cleaves the *B. subtilis* cell division protein FtsL (K. Chen and R. Zhou, unpublished results), their biological significance is under investigation. Knocking out these five $S2P_{Av}$ genes and characterizing the phenotypes of these five mutants are ongoing. The long-term goal is to understand the mechanisms of these $S2Ps_{Av}$ that govern RIPs and their biological significance in cyanobacteria.

ACKNOWLEDGMENTS

We thank Tom West for his critical reading of the manuscript. We also thank Eduardo Callegari at the University of South Dakota BRIN Proteomics Core Facility for performing Q-TOF mass spectrometry.

We acknowledge use of the South Dakota State University Functional Genomics Core Facility supported in part by NSF/EPSCoR grant 0091948 and by the State of South Dakota. This research was supported by NSF grant MCB0914691 (to R.Z.), DHHS/NIH FPT Undergraduate Research Subgrant (to R.Z. and M.L.) from grant number 2 P20 RR016479 (the National Center for Research Resources), and by the South Dakota Agricultural Experiment Station.

REFERENCES

1. **Adams DG, Duggan PS.** 1999. Tansley review no. 107. Heterocyst and akinete differentiation in cyanobacteria. New Phytol. **144**:3–33.
2. **Akiyama Y, Kanehara K, Ito K.** 2004. RseP (YaeL), an *Escherichia coli* RIP protease, cleaves transmembrane sequences. EMBO J. **23**:4434–4442.
3. **Alba BM, Leeds JA, Onufryk C, Lu CZ, Gross CA.** 2002. DegS and YaeL participate sequentially in the cleavage of RseA to activate the σ^E-dependent extracytoplasmic stress response. Genes Dev. **16**:2156–2168.
4. **Ali N, Knaüper V.** 2007. Phorbol ester-induced shedding of the prostate cancer marker transmembrane protein with epidermal growth factor and two follistatin motifs 2 is mediated by the disintegrin and metalloproteinase-17. J. Biol. Chem. **282**:37378–37388.
5. **Blot G, et al.** 2006. Luman, a new partner of HIV-1 TMgp41, interferes with Tat-mediated transcription of the HIV-1 LTR. J. Mol. Biol. **364**: 1034–1047.
6. **Bramkamp M, Weston L, Daniel RA, Errington J.** 2006. Regulated intramembrane proteolysis of FtsL protein and the control of cell division in *Bacillus subtilis*. Mol. Microbiol. **62**:580–591.
7. **Brown MS, Goldstein JL.** 1999. A proteolytic pathway that controls the cholesterol content of membranes, cells, and blood. Proc. Natl. Acad. Sci. U. S. A. **96**:11041–11048.
8. **Brown MS, Ye J, Rawson RB, Goldstein JL.** 2000. Regulated intramembrane proteolysis: a control mechanism conserved from bacteria to humans. Cell **100**:391–398.
9. **Campbell EL, Summers ML, Christman H, Martin ME, Meeks JC.** 2007. Global gene expression patterns of *Nostoc punctiforme* in steady-state dinitrogen-grown heterocyst-containing cultures and at single time points during the differentiation of akinetes and hormogonia. J. Bacteriol. **189**: 5247–5256.
10. **Chen JC, Viollier PH, Shapiro L.** 2005. A membrane metalloprotease participates in the sequential degradation of a *Caulobacter* polarity determinant. Mol. Microbiol. **55**:1085–1103.
11. **De Strooper B, et al.** 1999. A presenilin-1-dependent gamma-secretase-like protease mediates release of Notch intracellular domain. Nature **398**: 518.
12. **Dev KK, et al.** 2006. Signal peptide peptidase dependent cleavage of type II transmembrane substrates releases intracellular and extracellular signals. Eur. J. Pharmacol. **540**:10–17.
13. **Dong TC, Cutting SM.** 2004. The PDZ domain of the SpoIVB transmembrane signaling protein enables cis-trans interactions involving multiple partners leading to the activation of the Pro-σ^K processing complex in *Bacillus subtilis*. J. Biol. Chem. **279**:43468–43478.
14. **Ehira S, Ohmori M.** 2006. NrrA, a nitrogen-responsive response regulator facilitates heterocyst development in the cyanobacterium *Anabaena* sp. strain PCC 7120. Mol. Microbiol. **59**:1692–1703.
15. **Ellermeier CD, Losick R.** 2006. Evidence for a novel protease governing regulated intramembrane proteolysis and resistance to antimicrobial peptides in *Bacillus subtilis*. Genes Dev. **20**:1911–1922.
16. **Espenshade PJ, Li W-P, Yabe D.** 2002. Sterols block binding of COPII proteins to SCAP, thereby controlling SCAP sorting in ER. Proc. Natl. Acad. Sci. U. S. A. **99**:11694–11699.
17. **Feng L, et al.** 2007. Structure of a site-2 protease family intramembrane metalloprotease. Science **318**:1608–1612.
18. **Flaherty BL, Van Nieuwerburgh F, Head SR, Golden JW.** 2011. Directional RNA deep sequencing sheds new light on the transcriptional response of *Anabaena* sp. strain PCC 7120 to combined-nitrogen deprivation. BMC Genomics **12**:332. doi:10.1186/1471-2164-12-332.
19. **Freeman M.** 2004. Proteolysis within the membrane: rhomboids revealed. Nat. Rev. Mol. Cell Biol. **5**:188–197.
20. **Friedmann E, et al.** 2006. SPPL2a and SPPL2b promote intramembrane proteolysis of TNFα in activated dendritic cells to trigger IL-12 production. Nat. Cell Biol. **8**:843–848.
21. **Ghosh S, May MJ, Kopp EB.** 1998. NF-κB and rel proteins: evolutionarily conserved mediators of immune responses. Annu. Rev. Immunol. **16**: 225–260.
22. **Golden JW, Yoon H-S.** 2003. Heterocyst development in *Anabaena*. Curr. Opin. Microbiol. **6**:557–563.
23. **Gu W, Roeder RG.** 1997. Activation of p53 sequence-specific DNA binding by acetylation of the p53 C-terminal domain. Cell **90**:595–606.
24. **Guichard A, et al.** 1999. *rhomboid* and *Star* interact synergistically to promote EGFR/MAPK signaling during *Drosophila* wing vein development. Development **126**:2663–2676.
25. **Ignoul S, Eggermont J.** 2005. CBS domains: structure, function, and pathology in human proteins. Am. J. Physiol. Cell Physiol. **289**:C1369–C1378.
26. **Iwata Y, Koizumi N.** 2005. An *Arabidopsis* transcription factor, AtbZIP60, regulates the endoplasmic reticulum stress response in a manner unique to plants. Proc. Natl. Acad. Sci. U. S. A. **102**:5280–5285.
27. **Kaffman A, Herskowitz I, Tjian R, O'Shea E.** 1994. Phosphorylation of the transcription factor PHO4 by a cyclin-CDK complex, PHO80-PHO85. Science **263**:1153–1156.
28. **Kim Y-S, et al.** 2006. A membrane-bound NAC transcription factor regulates cell division in *Arabidopsis*. Plant Cell **18**:3132–3144.
29. **Kinch L, Ginalski K, Grishin N.** 2006. Site-2 protease regulated intramembrane proteolysis: sequence homologs suggest an ancient signaling cascade. Protein Sci. **15**:84–93.
30. **Krogh A, Larsson B, von Heijne G, Sonnhammer ELL.** 2001. Predicting transmembrane protein topology with a hidden Markov model: application to complete genomes. J. Mol. Biol. **305**:567–580.
31. **Kroos L, Yu Y-TN.** 2000. Regulation of σ factor activity during *Bacillus subtilis* development. Curr. Opin. Microbiol. **3**:553–560.
32. **Kroos L, Yu Y-TN, Mills D, Ferguson-Miller S.** 2002. Forespore signaling is necessary for pro-σ^K processing during *Bacillus subtilis* sporulation despite the loss of SpoIVFA upon translational arrest. J. Bacteriol. **184**: 5393–5401.
33. **Kroos L, Zhang B, Ichikawa H, Yu Y-TN.** 1999. Control of σ factor activity during *Bacillus subtilis* sporulation. Mol. Microbiol. **31**:1285–1294.
34. **Labrie C, et al.** 2008. Androgen-regulated transcription factor AIbZIP in prostate cancer. J. Steroid Biochem. Mol. Biol. **108**:237–244.
35. **Lal M, Caplan M.** 2011. Regulated intramembrane proteolysis: signaling pathways and biological functions. Physiology **26**:34–44.
36. **Leganés F.** 1994. Genetic evidence that *hepA* gene is involved in the normal deposition of the envelope of both heterocysts and akinetes in *Anabaena variabilis* ATCC 29413. FEMS Microbiol. Lett. **123**:63–67.
37. **Lemberg MK, Martoglio B.** 2004. On the mechanism of SPP-catalysed intramembrane proteolysis; conformational control of peptide bond hydrolysis in the plane of the membrane. FEBS Lett. **564**:213–218.
38. **Lewis AP, Thomas PJ.** 1999. A novel clan of zinc metallopeptidases with possible intramembrane cleavage properties. Protein Sci. **8**:439–442.
39. **Li T, et al.** 2007. Epidermal growth factor receptor and Notch pathways participate in the tumor suppressor function of γ-secretase. J. Biol. Chem. **282**:32264–32273.
40. **Makinoshima H, Glickman MS.** 2005. Regulation of *Mycobacterium tuberculosis* cell envelope composition and virulence by intramembrane proteolysis. Nature **436**:406–409.
41. **Makinoshima H, Glickman MS.** 2006. Site-2 proteases in prokaryotes: regulated intramembrane proteolysis expands to microbial pathogenesis. Microbes Infect. **8**:1882–1888.
42. **Matson JS, DiRita VJ.** 2005. Degradation of the membrane-localized virulence activator TcpP by the YaeL protease in *Vibrio cholerae*. Proc. Natl. Acad. Sci. U. S. A. **102**:16403–16408.
43. **Meeks JC.** 2003. Symbiotic interactions between *Nostoc punctiforme*, a multicellular cyanobacterium, and the hornwort *Anthoceros punctatus*. Symbiosis **35**:55–71.
44. **Meeks JC, Elhai J.** 2002. Regulation of cellular differentiation in filamentous cyanobacteria in free-living and plant-associated symbiotic growth states. Microbiol. Mol. Biol. Rev. **66**:94–121.
45. **Okamoto K, Moriishi K, Miyamura T, Matsuura Y.** 2004. Intramembrane proteolysis and endoplasmic reticulum retention of hepatitis C virus core protein. J. Virol. **78**:6370–6380.
46. **Rai A.** 1990. Handbook of symbiotic cyanobacteria. CRC Press, Inc., Boca Raton, FL.
47. **Rawson RB.** 2003. The SREBP pathway—insights from insigs and insects. Nat. Rev. Mol. Cell Biol. **4**:631–640.
48. **Rudner DZ, Fawcett P, Losick R.** 1999. A family of membrane-embedded metalloproteases involved in regulated proteolysis of membrane-associated transcription factors. Proc. Natl. Acad. Sci. U. S. A. **96**: 14765–14770.
49. **Saribas AS, Gruenke L, Waskell L.** 2001. Overexpression and purification of the membrane-bound cytochrome P450 2B4. Protein Expr. Purif. **21**: 303–309.
50. **Schöbel S, Zellmeier S, Schumann W, Wiegert T.** 2004. The *Bacillus subtilis* σ^W anti-sigma factor RsiW is degraded by intramembrane proteolysis through YluC. Mol. Microbiol. **52**:1091–1105.

51. **Selkoe D, Kopan R.** 2003. Notch and presenilin: regulated intramembrane proteolysis links development and degeneration. Annu. Rev. Neurosci. **26**:565–597.
52. **Shen J, Prywes R.** 2004. Dependence of site-2 protease cleavage of ATF6 on prior site-1 protease digestion is determined by the size of the luminal domain of ATF6. J. Biol. Chem. **279**:43046–43051.
53. **Steiner H, Haass C.** 2000. Intramembrane proteolysis by presenilins. Nat. Rev. Mol. Cell Biol. **1**:217–224.
54. **Sturtevant MA, Roark M, Bier E.** 1993. The *Drosophila* rhomboid gene mediates the localized formation of wing veins and interacts genetically with components of the EGF-R signaling pathway. Genes Dev. **7**:961–973.
55. **Sun L-P, Li L, Goldstein JL, Brown MS.** 2005. Insig required for sterol-mediated inhibition of Scap/SREBP binding to COPII proteins in vitro. J. Biol. Chem. **280**:26483–26490.
56. **Urban S.** 2009. Making the cut: central roles of intramembrane proteolysis in pathogenic microorganisms. Nat. Rev. Microbiol. **7**:411–423.
57. **Urban S, Freeman M.** 2002. Intramembrane proteolysis controls diverse signalling pathways throughout evolution. Curr. Opin. Genet. Dev. **12**: 512–518.
58. **Wang Y, Zhang Y, Ha Y.** 2006. Crystal structure of a rhomboid family intramembrane protease. Nature **444**:179–180.
59. **Weihofen A, Martoglio B.** 2003. Intramembrane-cleaving proteases: controlled liberation of proteins and bioactive peptides. Trends Cell Biol. **13**:71–78.
60. **Wild-Bode C, Fellerer K, Kugler J, Haass C, Capell A.** 2006. A basolateral sorting signal directs ADAM10 to adherens junctions and is required for its function in cell migration. J. Biol. Chem. **281**:23824–23829.
61. **Wolfe MS, Kopan R.** 2004. Intramembrane proteolysis: theme and variations. Science **305**:1119–1123.
62. **Wolk CP.** 1996. Heterocyst formation. Annu. Rev. Genet. **30**:59–78.
63. **Wolk CP.** 2000. Heterocyst formation in *Anabaena*, p 83–104. *In* Brun VV, Shimkets LJ (ed), Prokaryotic development. ASM Press, Washington, DC.
64. **Wood LF, Leech AJ, Ohman DE.** 2006. Cell wall-inhibitory antibiotics activate the alginate biosynthesis operon in *Pseudomonas aeruginosa*: roles of σ^{22} (AlgT) and the AlgW and Prc proteases. Mol. Microbiol. **62**:412–426.
65. **Ye J, et al.** 2000. ER stress induces cleavage of membrane-bound ATF6 by the same proteases that process SREBPs. Mol. Cell **6**:1355–1364.
66. **Yu YT, Kroos L.** 2000. Evidence that SpoIVFB Is a novel type of membrane metalloprotease governing intercompartmental communication during *Bacillus subtilis* sporulation. J. Bacteriol. **182**:3305–3309.
67. **Zhou R, Cusumano C, Sui D, Garavito RM, Kroos L.** 2009. Intramembrane proteolytic cleavage of a membrane-tethered transcription factor by a metalloprotease depends on ATP. Proc. Natl. Acad. Sci. U. S. A. **106**: 16174–16179.
68. **Zhou R, Kroos L.** 2004. BofA protein inhibits intramembrane proteolysis of pro-σ^K in an intercompartmental signaling pathway during *Bacillus subtilis* sporulation. Proc. Natl. Acad. Sci. U. S. A. **101**:6385–6390.
69. **Zhou R, Kroos L.** 2005. Serine proteases from two cell types target different components of a complex that governs regulated intramembrane proteolysis of pro-σ^K during *Bacillus subtilis* development. Mol. Microbiol. **58**:835–846.
70. **Zhou R, Wolk CP.** 2002. Identification of an akinete marker gene in *Anabaena variabilis*. J. Bacteriol. **184**:2529–2532.